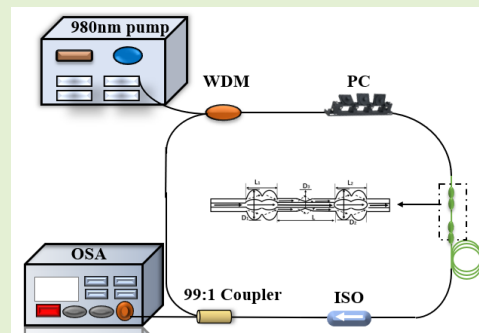


Temperature Sensor Based on Er-Doped Cascaded-Peanut Taper Structure In-Line Interferometer in Fiber Ring Laser

Weihao Lin¹, Fang Zhao, Li-Yang Shao¹, Senior Member, IEEE, Mang I. Vai, Senior Member, IEEE, Perry Ping Shum², Senior Member, IEEE, and Siming Sun

Abstract—A temperature sensor based on erbium-doped fiber cascaded peanut taper (EDFCPT) structure in fiber ring laser (FRL) cavity is proposed and studied. The cascaded peanut structure was fabricated by erbium-doped fiber. The cladding mode and core mode interference and the strong thermo-optical effect of erbium-doped fiber were used to realize the high sensitivity measurement of temperature. The mode interference and thermal sensitivity effects of EDFCPT in a broadband super-continuous light source and a fiber ring laser cavity were studied and compared experimentally. Besides, Erbium-doped fiber cascaded peanut (EDFCP) structure was designed to compare performance with EDFCPT. The experimental results show that EDFCPT has a higher signal to noise ratio (SNR) ($\sim 50\text{dB}$) and a narrower 3-dB bandwidth ($\sim 0.12\text{nm}$) than the broadband light source. Among them, the temperature sensitivity of EDFCPT is $571\text{pm}/^\circ\text{C}$ which is two times higher than the EDFCP ($\sim 249\text{nm}/^\circ\text{C}$) structure at range from 5°C – 55°C . The proposed temperature sensor has the advantages of high sensitivity, good repeatability, simple fabrication, compact structure, etc. It has a good application prospect in the field of aerospace and life health monitoring.

Index Terms—Temperature sensor, erbium-doped fiber double peanut taper, fiber ring laser.



I. INTRODUCTION

TEMPERATURE sensing is of great significance for many practical applications including monitoring of human body temperature and real-time monitoring of ambient temperature for cell culture, etc. Compared with the traditional sensors, the optical fiber sensor has the characteristics of small weight, immunity to electromagnetic interference, anti-corrosion, high precision and so on. The application scope of optical fiber sensors has penetrated into the fields of health

monitoring, civil engineering, oil well monitoring [1]–[3], etc. It can realize the measurement of physical quantities such as temperature [4], refractive index [5], electric field [6], magnetic field [7], cells [8] and so on. The research of optical fiber temperature sensor is in the ascence and has a broad development prospect.

Manuscript received August 11, 2021; accepted August 12, 2021. Date of publication August 17, 2021; date of current version October 1, 2021. This work was supported by a startup fund from the Southern University of Science and Technology and Shenzhen Government. The associate editor coordinating the review of this article and approving it for publication was Dr. Santosh Kumar. (Corresponding author: Li-Yang Shao.)

Weihao Lin, Fang Zhao, Li-Yang Shao, Perry Ping Shum, and Siming Sun are with the Department of Electrical and Electronic Engineering, Southern University of Science and Technology, Shenzhen 518055, China (e-mail: 11510630@mail.sustech.edu.cn; 12031197@mail.sustech.edu.cn; shaoly@sustech.edu.cn; shenp@sustech.edu.cn; simingsun@163.com).

Mang I. Vai is with the Department of Electrical and Computer Engineering, Faculty of Science and Technology, University of Macau, Macau, China (e-mail: fstmiv@um.edu.mo).

Digital Object Identifier 10.1109/JSEN.2021.3105408

At present, optical fiber sensor devices used in temperature testing mainly include fiber Bragg grating (FBG) [9], [10] photonic crystal fiber (PCF) [11] tilted fiber grating [12], etc. Among them, the Mach-Zehnder interferometer (MZI) structure sensor based on the FBG has higher requirements for the writing technology of FBG. Besides, PCF based sensor has high production cost, relatively complex structure, low repeatability. In order to improve the sensitivity of the fiber temperature sensor, structures including tapering and polishing single-mode fiber have been proposed. In 2015, Qian *et al.* [13] proposed a method by using standard communication single-mode fiber to fabricate cascaded peanut junction, and its temperature sensing sensitivity was $63.7\text{pm}/^\circ\text{C}$. Wu *et al.* [14] proposed a Michelson interferometer based on fiber peanut junction. The temperature sensitivity of the sensor is $96\text{pm}/^\circ\text{C}$. In 2013, Zhang *et al.* [15] proposed a curved single-mode multi-mode structure fixed on a polymer plate with a temper-

ature sensitivity of 6.5nm/°C. However, with the increasing demand for practical applications. It is of practical significance to realize the optical fiber temperature sensor with high signal-to-noise ratio, narrow 3-dB bandwidth and high sensitivity.

Thanks to the characteristics of fiber ring laser, fiber ring laser sensor can overcome the limitations of low resolution and low detection power, improve the detection SNR, to improve the sensing accuracy. In 2015, Gonzalez-Reyna *et al.* [16] experimentally demonstrated a laser-based temperature sensor using the MZI and grating. Temperature sensitivity of about 18.8pm/°C can be achieved. In 2017, Yang *et al.* [17] achieved a high sensitivity temperature detection using a liquid-filled photonic crystal fiber laser with a sensitivity of 1.747nm/°C. In 2020, Shi *et al.* [18] proposed an ultra-high resolution laser temperature sensor with an improved resolution from 10^{-3} to 10^{-6} using FBG and Sagnac rings. However, all the above sensors require additional sensor heads as filters, increasing system costs and reducing stability.

In this paper, an erbium-doped fiber cascaded peanut taper-based temperature sensor in a FRL cavity is proposed and experimentally demonstrated. The erbium-doped fiber with strong thermo-optical effect is used to enhance the sensitivity of the cascaded peanut structure internal mode interference to realize high sensitivity measurement of temperature. Besides, based on the characteristics of the laser, high SNR and narrow 3dB bandwidth are achieved. Different from the traditional FRL sensor, the designed structure does not need additional sensing head and filter. Effectively improve the system stability and accuracy. Moreover, Erbium-doped fibers have another two advantages as sensing units. First, there is no need to design additional filters to improve the stability of the system. Finally, the fiber is not only the sensing unit, but also the gain medium, reducing the cost of the whole system. The experimental results show that the sensitivity of the sensor based on EDFCP and EDFCPT are 249pm/°C and 571pm/°C, respectively. the FRL temperature sensor based on EDFCPT structure has the advantages of high sensitivity, low cost, simple manufacture, compact structure which make it has potential application value in remote temperature detection and sea water temperature calibration and other fields.

II. SENSOR SETUP AND PRINCIPLE

Fig.1 is the schematic diagram of the designed temperature sensor structure based on EDFCPT. EDFCPT is composed of two cascade erbium-doped fiber peanut structures, the connecting part of which is tapered. Each peanut junction structure is interfered by two erbium-doped fiber core mode and cladding modes. The light field is transmitted through the first rare earth fiber to the first peanut junction. Firstly, the light field is transmitted in the core in the form of a core mode (shown by the arrow of the thick solid line). When the light field passes through the first microsphere, the cladding mode (dotted arrow) is excited due to the mismatch of core diameter. and the light field is further transmitted to the second microsphere. At the junction of the second microsphere and the rare earth fiber, some higher-order cladding modes are re-coupled into the fiber core, and then propagate along the fiber core and interfere with the core mode simultaneously. The process of

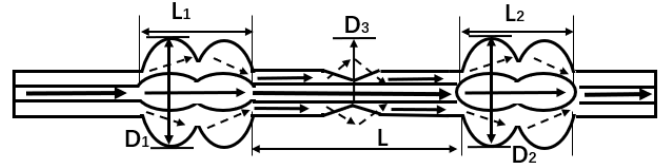


Fig. 1. Schematic of fiber temperature sensor based on EDFCPT.

light field transmission in the taper region and second peanut structure is the same as that in the first peanut structure. Since different modes have different phases, there will be phase difference between modes. The cladding mode power can be improved effectively by tapering the fiber in the region between two peanut structures.

In Fig.1, the output light intensity after the interference between the core mode and the cladding mode in the second peanut structure can be expressed as [16]:

$$I = I_1 + I_2 + 2\sqrt{I_1 I_2} \cos \left[2\pi L \left(n_{cl}^{eff} - \frac{n_{cm,n}^{eff}}{\lambda} \right) \right] \quad (1)$$

where, I_1, I_2 refers to the light intensity of core mode and cladding mode respectively. The wavelength of the transmitted light is λ . L is the coherence length; The effective refractive index of core mode is n_{cl}^{eff} and that of cladding mode is $n_{cm,n}^{eff}$. Since different propagation constants between different modes, phase difference will occur between different modes after the transmission phase separation. In EDFCPT, multi-order cladding modes excited into cladding participate in interference, and different order cladding modes correspond to different effective refractive index. The phase difference between core mode and cladding modes $\Delta\phi$ is [14]:

$$\Delta\phi = 2\pi L \left(n_{cl}^{eff} - n_{cm,n}^{eff} \right) / \lambda \quad (2)$$

the wavelength can be obtained by equation (2) as:

$$\lambda_{dip} = 2L \left(n_{cl}^{eff} - n_{cm,n}^{eff} \right) / (2m + 1) \quad (3)$$

When m is an integer, the interference intensity is the smallest. Since the cladding refractive index of the sensor matches the external temperature and the core is not in contact with the outside, the effective refractive index of the cladding mode is not only related to the incident wavelength of the transmitted light, but also related to the external temperature, while the effective refractive index of the core mode is only related to the incident wavelength of the transmitted light.

When the external temperature changes, Δn_{eff} changes, resulting in wavelength drift. Wavelength drift of interference spectrum can be expressed as [14]:

$$\Delta\lambda \approx 2\lambda \left[\frac{1}{\Delta n_{eff}} \delta + k \right] \Delta T \quad (4)$$

where, δ is the number of thermal-optical system of optical fiber; k is the thermal expansion coefficient of optical fiber. The change of temperature affects the wavelength of interference spectrum through thermal-light effect and thermal

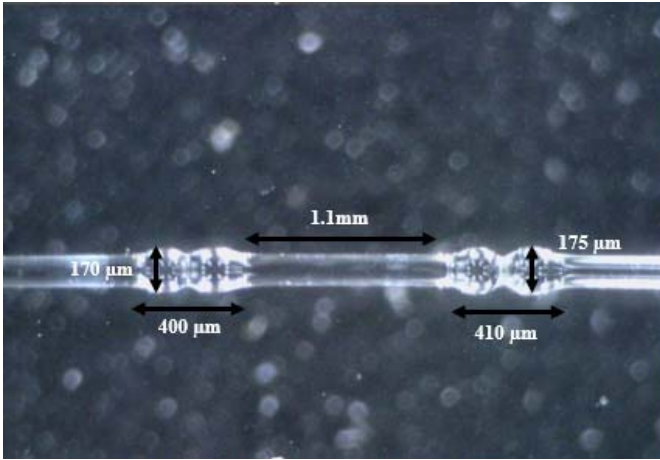


Fig. 2. Microscopic image of the Er-doped double peanut-shaped structure.

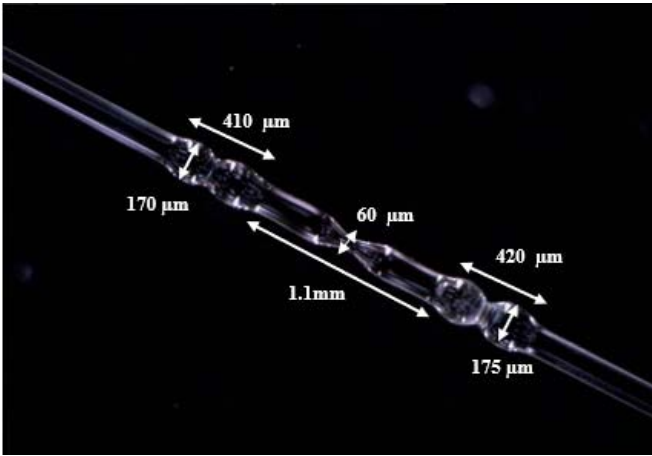


Fig. 3. Schematic diagram of Er-doped peanut-shaped fiber structure sensor.

expansion effect. δ and k can be expressed as:

$$\delta = \frac{dn_{eff}^{core}}{dT} - \frac{dn_{eff}^{clad,m}}{dT} \quad (5)$$

$$k = \frac{1}{L} \frac{dL}{dT} \quad (6)$$

As can be seen from Equation (6), compared with ordinary single-mode fiber, the erbium ion in erbium-doped fiber makes the proposed EDFCPT have stronger thermo-optical effect and can effectively improve its temperature sensing sensitivity.

Fig.2 and Fig.3 show the actual microscope photos of the EDFCPT structure and the tapered cascade peanut junction structure prepared in the experiment. In the experiment, EDFCPT is made by the method of arc discharge of optical fiber fusion splicer, and the discharge time and current of splicer are determined the key parameters of EDFCPT. The specific steps are as follows: first, the erbium-doped fiber is stripped of the coating layer and wiped clean with alcohol. Then, the fiber end is cut flat with an optical fiber cutter. Then place the two fiber ends cut flat in the optical fiber welding machine respectively, and make it in the state to be fused. Adjust the two fiber ends to the appropriate position, and the two end faces can be seen on the plane of the

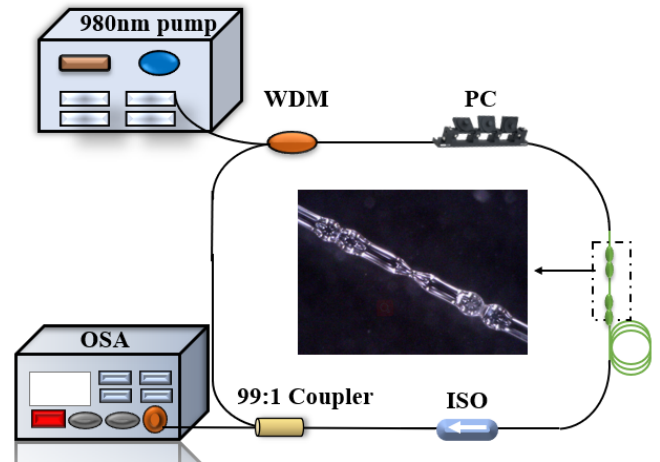


Fig. 4. The intracavity sensing system based on FRL.

optical fiber welding machine. Set the discharge power and discharge time, discharge, the two end faces are softened by heat, because of the surface tension of the material itself, the fused fiber end face gradually tends to arc shape in the cooling process. Using the manual motor drive function of the optical fiber welding machine. Drive the motors on the left and right sides to make the arc-shaped optical fiber end surfaces of the dipping liquid body contact. Then the driving motors on the left and right sides are simultaneously promoted, and the micro-displacement is applied to the optical fiber contact. Precision discharge stage. The main stage is discharge welding. Firstly, the discharge time and the discharge time are adjusted, the "standard" power rate is generally selected, the discharge time is selected 800 ms, and then the discharge is repeated for 10 times and the optical fiber peanut structure size is observed through the interface of the optical fiber welding machine. The section of optical fiber is fused into a spherical lens near its end face because of surface tension. Another spherical lens is prepared by the same method, the two spherical lenses are placed in the welding machine. At the same time, the position, and the distance between the two are adjusted, and the discharge welding is carried out again. After that a single spherical structure is obtained. Finally, two single spheres are fused together to form two cascaded EDFCPT structure. The structural parameters of EDFCPT are as follows: $D_1 = 170\mu\text{m}$, $D_2 = 175\mu\text{m}$, $D_3 = 60\mu\text{m}$, $L_1 = 410\mu\text{m}$, $L_2 = 420\mu\text{m}$; $L = 1.1\text{mm}$. The sensor head design in this system costs less than \$5, much less than the gold-coated Fabry-Perot cavity and liquid-filled photonic crystal fibers.

The schematic diagram of the experimental device is shown in Figure 4. The laser emitted by the 980nm (PL-974-500-FC/APC-P-M) diode is pumped through the WDM into the FRL cavity. The polarization controller is used to control the polarization state of the laser. EDFCPT is used as gain medium, filter and sensing head, simultaneously. The total length of erbium-doped fiber is 1.6m. The isolator is used to control the unidirectional transmission of light, and 1% of the light is transmitted through a 99:1 coupler to a 0.02nm optical spectrum analyzer (Yokogawa AQ6370D) for detecting the signal output.

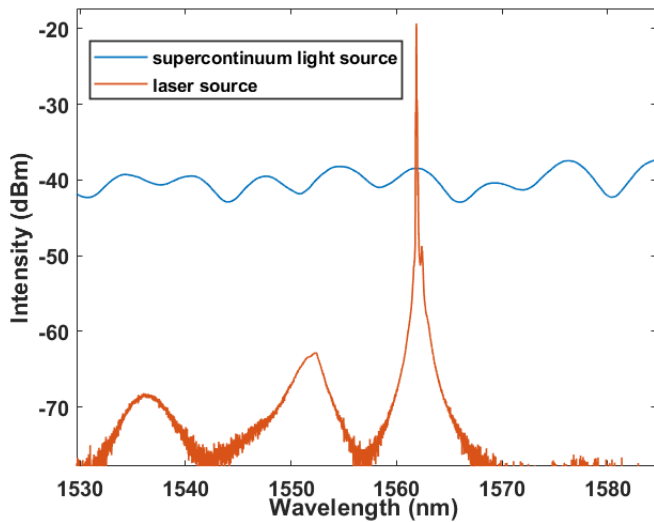


Fig. 5. Transmission spectra of the EDFCPT under supercontinuum light source (blue line) and the proposed fiber ring laser (orange line).

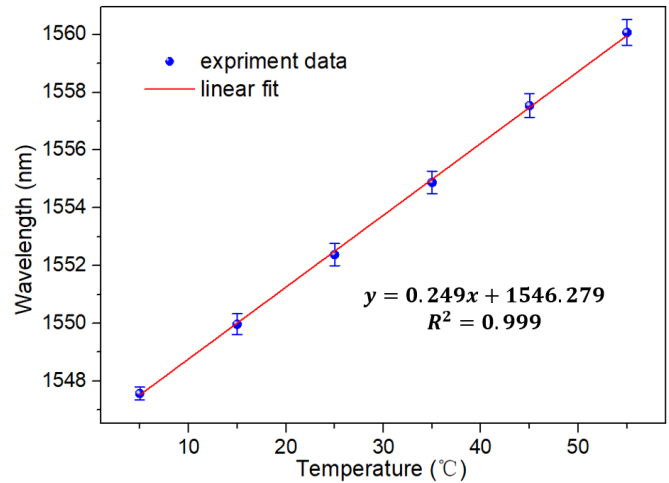


Fig. 7. Linear fitting and error bars of the relationship between temperature and wavelength shift in Erbium-doped fiber double peanut structure.

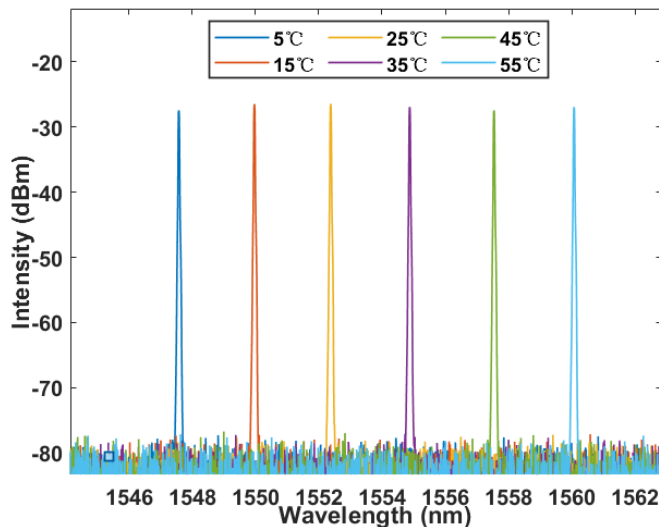


Fig. 6. Spectral response at different temperatures for erbium-doped fiber double peanut structure.

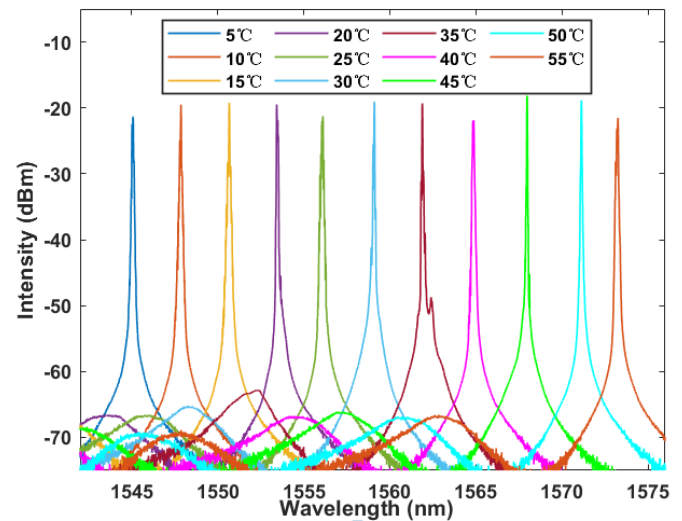


Fig. 8. Spectral response at different temperatures for Erbium-doped fiber tapered double peanut structure.

In this case, erbium-doped fiber be used as the sensing unit has three advantages. First, there is no need to design additional filters, simplifying the system and reducing the cost. Secondly, the thermal expansion coefficient of erbium-doped fiber is larger than that of single-mode fiber, which improves the sensitivity. Finally, erbium-doped fiber can also be used as gain medium to improve the stability of the system.

III. EXPERIMENTAL RESULTS AND DISCUSSION

Fig.5 shows the correspondence between the super-continuous source and the FRL. At 30°C, the laser peak of FRL is in good agreement with the interference peak of super continuous light source.

To further demonstrate the sensitivity of EDFCPT structure. The temperature experimental results of erbium-doped fiber double peanut structure with almost identical parameters with

EDFCPT are demonstrated at first. The test results are shown in Fig.6 and Fig.7. In the range of 5°C-55°C, the wavelength shifts to the long wavelength direction as the temperature increases. The detection sensitivity was 0.249nm/°C, with linearity up to 0.999.

As shown in Fig.8 and Fig.9, the measured temperature ranges from 5 °C to 55 °C. As the temperature increases, the laser wavelength moves to the long wavelength direction, and the wavelength redshifts. The temperature sensitivity was 0.571nm/°C, and the corresponding linear fitting coefficient was 0.999. The migration of single peak output wavelength is well linear fitting to temperature. In addition, the sensor has a signal-to-noise ratio of 50dB and a 3-dB bandwidth of less than 0.12nm. At 30°C, the wavelength stability and power fluctuation of the sensor are shown in Figure 10. It is used to quantitatively analyze the stability of FRL sensor system. In 2.5 hours, the wavelength deviation is 0.1nm and

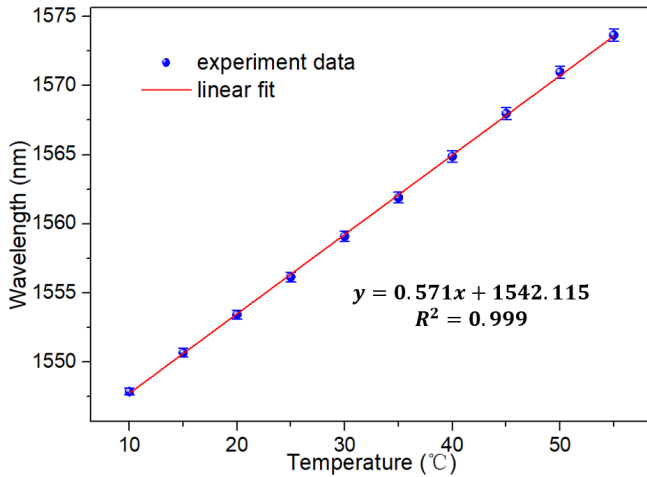


Fig. 9. Linear fitting and error bars of the relationship between temperature and wavelength shift in Erbium-doped fiber tapered double peanut structure.

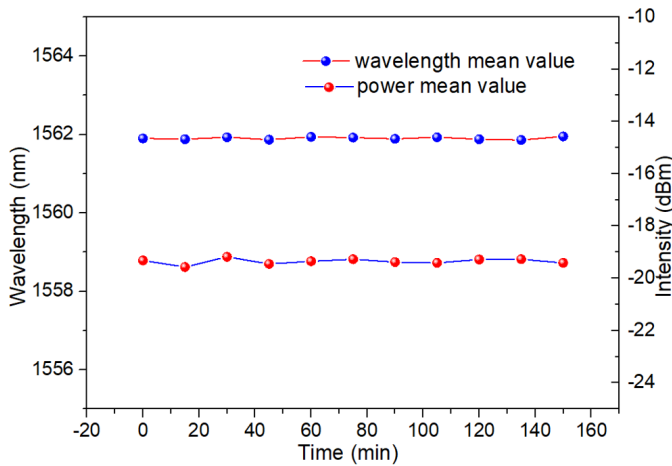


Fig. 10. Test for time stability of wavelength shift and power fluctuation.

TABLE I
SENSITIVITY COMPARISON WITH OTHER
TEMPERATURE SENSING STRUCTURES

Structures	Sensitivity(p m/°C)	Refs.
Er doped MZI	157	[17]
Offset Mach-Zehnder interferometer	49	[18]
STCS fiber structure	11	[19]
FP air cavity between two SMFs	249	[20]
Current work	571	

the intensity change is less than 0.5 dBm. This shows the reliability and stability of the system as a sensor.

Besides, Table I compares the performance of the temperature sensor with other structures. It is verified that the designed sensor has good temperature sensing performance except without additional filter.

IV. CONCLUSION

A temperature sensing based on the EDFCPT sensor and FRL system is proposed. The EDFCPT based MZI is inserted

into the FRL as sensing element, gain medium and filter. Therefore, in addition to high sensitivity to the surrounding environment, the sensor system also effectively reduces the system cost and improves the reliability. The sensor demonstrated excellent temperature sensing characteristics with a sensitivity of 571pm/°C. Besides, the signal-to-noise ratio of the FRL sensing system is 50dB, and the 3dB bandwidth is less than 0.15nm. In addition, EDFCPT has the advantages of good mechanical strength, simple manufacture, and low sensing cost, which makes it attractive for life health detection and ocean temperature detection.

REFERENCES

- [1] H. Fu, S. Zhang, H. Chen, and J. Weng, "Graphene enhances the sensitivity of fiber-optic surface plasmon resonance biosensor," *IEEE Sensors J.*, vol. 15, no. 10, pp. 5478–5482, Oct. 2015.
- [2] E. Leviatan and A. Eyal, "High resolution DAS via sinusoidal frequency scan OFDR (SFS-OFDR)," *Opt. Exp.*, vol. 23, no. 26, pp. 33318–33334, Dec. 2015.
- [3] R. Goldman, A. Agmon, and M. Nazarathy, "Direct detection and coherent optical time-domain reflectometry with Golay complementary codes," *J. Lightw. Technol.*, vol. 31, no. 13, pp. 2207–2222, Jul. 1, 2013.
- [4] W. Lin *et al.*, "Temperature sensor based on fiber ring laser with cascaded fiber optic Sagnac interferometers," *IEEE Photon. J.*, vol. 13, no. 2, pp. 1–12, Apr. 2021.
- [5] J. Wang *et al.*, "Liquid refractive index sensor based on a polarization-maintaining fiber loop mirror," *IEEE Sensors J.*, vol. 13, no. 5, pp. 1721–1724, May 2013.
- [6] S. Mathews, G. Farrell, and Y. Semenova, "All-fiber polarimetric electric field sensing using liquid crystal infiltrated photonic crystal fibers," *Sens. Actuators A, Phys.*, vol. 167, no. 1, pp. 54–59, May 2011.
- [7] C. Yue, H. Ding, and X. Liu, "Magnetic-field measurement based on multicore fiber taper and magnetic fluid," *IEEE Trans. Instrum. Meas.*, vol. 68, no. 3, pp. 688–692, Mar. 2019.
- [8] D. Sun, Y. Ran, and G. Wang, "Label-free detection of cancer biomarkers using an in-line taper fiber-optic interferometer and a fiber Bragg grating," *Sensors*, vol. 17, no. 11, p. 2559, Nov. 2017.
- [9] C.-Y. Hsu, C.-C. Chiang, T.-S. Hsieh, H.-C. Hsu, L. Tsai, and C.-H. Hou, "Study of fiber Bragg gratings with TiN-coated for cryogenic temperature measurement," *Opt. Laser Technol.*, vol. 136, Apr. 2021, Art. no. 106768.
- [10] S. Ju, P. R. Watekar, and W.-T. Han, "Enhanced sensitivity of the FBG temperature sensor based on the PbO-GeO₂-SiO₂ glass optical fiber," *J. Lightw. Technol.*, vol. 28, no. 18, pp. 2697–2700, Sep. 15, 2010.
- [11] W. Qian *et al.*, "Temperature sensing based on ethanol-filled photonic crystal fiber modal interferometer," *IEEE Sensors J.*, vol. 12, no. 8, pp. 2593–2597, Aug. 2012.
- [12] S. Bandyopadhyay *et al.*, "Highly efficient free-space fiber coupler with 45 degrees tilted fiber grating to access remotely placed optical fiber sensors," *Opt. Exp.*, vol. 28, no. 11, pp. 16569–16578, May 25 2020.
- [13] Z. Qian, H. Gong, X. Yang, K. Ni, C.-L. Zhao, and X. Dong, "Optical fiber temperature sensor based on modal interferometer comprising two peanut-shape structures," *Microw. Opt. Technol. Lett.*, vol. 57, no. 12, pp. 2841–2844, Dec. 2015.
- [14] D. Wu, T. Zhu, and M. Liu, "A high temperature sensor based on a peanut-shape structure Michelson interferometer," *Opt. Commun.*, vol. 285, no. 24, pp. 5085–5088, 2012.
- [15] Y. Zhang, X. Tian, L. Xue, Q. Zhang, L. Yang, and B. Zhu, "Super-high sensitivity of fiber temperature sensor based on leaky-mode bent SMS structure," *IEEE Photon. Technol. Lett.*, vol. 25, no. 6, pp. 560–563, Mar. 15, 2013.
- [16] M. A. Gonzalez-Reyna *et al.*, "Laser temperature sensor based on a fiber Bragg grating," *IEEE Photon. Technol. Lett.*, vol. 27, no. 11, pp. 1141–1144, Jun. 1, 2015.
- [17] X. Yang, Y. Lu, B. Liu, and J. Yao, "Fiber ring laser temperature sensor based on liquid-filled photonic crystal fiber," *IEEE Sensors. J.*, vol. 17, no. 21, pp. 6948–6952, Nov. 2017.

- [18] J. Shi *et al.*, “High-resolution temperature sensor based on intracavity sensing of fiber ring laser,” *J. Lightw. Technol.*, vol. 38, no. 7, pp. 2010–2014, Apr. 1, 2020.
- [19] M. Sun, Y. Jin, and X. Dong, “All-fiber Mach–Zehnder interferometer for liquid level measurement,” *IEEE Sensors J.*, vol. 15, no. 7, pp. 3984–3988, Jul. 2015.
- [20] W. Lin *et al.*, “In-fiber Mach–Zehnder interferometer sensor based on er doped fiber peanut structure in fiber ring laser,” *J. Lightw. Technol.*, vol. 39, no. 10, pp. 3350–3357, May 15, 2021.
- [21] L. Cai, Y. Zhao, and X.-G. Li, “A fiber ring cavity laser sensor for refractive index and temperature measurement with core-offset modal interferometer as tunable filter,” *Sens. Actuators B, Chem.*, vol. 242, pp. 673–678, Apr. 2017.
- [22] L. Liang, G. Ren, B. Yin, W. Peng, X. Liang, and S. Jian, “Refractive index and temperature sensor based on fiber ring laser with STCS fiber structure,” *IEEE Photon. Technol. Lett.*, vol. 26, no. 21, pp. 2201–2204, Nov. 1, 2014.
- [23] H. Zou, L. Ma, H. Xiong, Y. Zhang, and Y. T. Li, “Fiber ring laser sensor based on Fabry–Pérot cavity interferometer for temperature sensing,” *Laser Phys.*, vol. 28, no. 1, Jan. 2018, Art. no. 015102.

Weihao Lin received the B.Eng. degree in optoelectronic information science and engineering from the Southern University of Science and Technology, China, in 2019. He is currently pursuing the joint Ph.D. degree under a collaboration program between the Southern University of Science and Technology and the University of Macau. His research interests include optical fiber sensors, fiber laser sensors, and fiber lasers.

Fang Zhao is currently pursuing the Ph.D. degree in electronic and electrical engineering with the Southern University of Science and Technology, China.



Li-Yang Shao (Senior Member, IEEE) received the Ph.D. degree in optical engineering from Zhejiang University, China, in 2008. From 2006 to 2009, he was with The Hong Kong Polytechnic University as a Research Assistant/Associate, working on fiber grating devices and sensors. Then, he was a Postdoctoral Fellow with the Department of Electronics, Carleton University, Canada. In 2011, he returned to The Hong Kong Polytechnic University for another Postdoctoral Research Project. In 2012, he was granted the Endeavor Research Fellowship from the Australian Government and worked with the Interdisciplinary Photonics Laboratory, University of Sydney. In 2013, he joined Southwest Jiaotong University as a Full Professor. In 2017, he joined the Department of Electrical and Electronic Engineering, Southern University of Science and Technology, where he became the Associate Dean of the School of Innovation and Entrepreneurship in 2018. He has authored/coauthored more than 150 articles in refereed international journals/conferences with a total citation of more than 2800 times (SCI citation of over 1800 times by other researchers). His research interests include fiber grating and sensors, distributed fiber optic sensing, microwave photonics for sensing, and smart sensing systems for railway industry. He acts as the Principal Investigator for several high-level projects, such as NSFC projects, International S&T Cooperation Program of China, etc. He was a TPC or Organizing Committee Member of multiple conferences, including ICAIT (2009–2013), PGC 2010, OFS 2011, PIERS 2014, ICOCN (2015–2016), PGC 2017, APOS 2018, CLEO-PR 2018, ACP 2019, APOS 2019, and CLEO-PR 2020. He serves as a Reviewer for more than 20 SCI journals, including *Optics Letters*, *Optics Express*, the *Journal of Lightwave Technology*, and the IEEE PHOTONICS TECHNOLOGY LETTERS.

Mang I. Vai (Senior Member, IEEE) received the Ph.D. degree in electrical and electronics engineering from the University of Macau, China, in 2002.

He is currently a Coordinator of the State Key Laboratory of Analog and Mixed-Signal VLSI and an Associate Professor of Electrical and Computer Engineering with the Faculty of Science and Technology, University of Macau. Since 1984, he has been performing research in the areas of digital signal processing and embedded systems.

Perry Ping Shum (Senior Member, IEEE) received the B.Eng. and Ph.D. degrees in electronic and electrical engineering from the University of Birmingham, Birmingham, U.K., in 1991 and 1995, respectively. In 1999, he joined the School of Electrical and Electronic Engineering, Nanyang Technological University, Nanyang, China. He has authored or coauthored more than 400 international journal and conference papers. His research interests are concerned with optical communications, fiber sensors, and fiber lasers. He is the technical program chair, committee member, and international advisor of many international conferences.

Siming Sun received the B.Eng. degree in optoelectronic information science and engineering from Huazhong University of Science and Technology, China, in 2020. He is currently pursuing the MA.Eng. degree with the Southern University of Science and Technology.